0026-895X/08/7306-1622–1631$20.00
MOLECULAR PHARMACOLOGY
Copyright © 2008 The American Society for Pharmacology and Experimental Therapeutics
Mol Pharmacol 73:1622–1631, 2008

Vol. 73, No. 6
43182/3339181
Printed in U.S.A.

Protease-Activated Receptor-1 Mediates Thrombin-Induced Persistent Sodium Current in Human Cardiomyocytes

Caroline Pinet,[1] Vincent Algalarrondo, Sylvie Sablayrolles, Bruno Le Grand, Christophe Pignier, Didier Cussac, Michel Perez, Stephane N. Hatem, and Alain Coulombe

Centre National de la Recherche Scientifique, Unité 8162, Université de Paris XI, and Laboratoire de Recherches Médicales, Hôpital Marie Lannelongue, Le Plessis-Robinson, France (C.P.); Institut National de la Santé et de la Recherche Médicale, Unité 621, and Université Pierre et Marie Curie-Paris 6, Unité Mixte de Recherche S621, Paris, France (V.A., S.N.H., A.C.); and Division of Cardiovascular Diseases II, Centre de Recherche Pierre Fabre, Castres, France (S.S., B.LG, C.P., D.C., M.P.)

Received November 5, 2007; accepted March 6, 2008

ABSTRACT

After the thrombus formation in cardiac cavities or coronaries, the serine protease thrombin is produced and can therefore reach the myocardial tissue by the active process of extravasation and binds to the G protein-coupled protease-activated receptor-1 (PAR1) expressed in human myocardium. The role of PAR1 was investigated in the thrombin effect on sodium current (I_{Na}). I_{Na} was recorded in freshly isolated human atrial myocytes by the whole-cell patch-clamp method. Action potentials (AP) were recorded in guinea pig ventricular tissue by the conventional glass microelectrode technique. Thrombin-activated PAR1 induced a tetrodotoxin-blocked persistent sodium current, I_{NaP}, in a concentration-dependent manner with an apparent EC_{50} of 28 U/ml. The PAR1 agonist peptide SFLLR-NH_2 (50 μM) was able to mimic PAR1-thrombin action, whereas PAR1 antagonists N^3-cyclopropyl-7-((4-(1-methylethyl)-phenyl)methyl)-7*H*-pyrrolo(3,2-*f*)quinazoline-1,3-diamine (SCH 203099; 10 μM) and 1-(3,5-di-*tert*-butyl-4-hydroxy-phenyl)-2-[3-(3-ethyl-3-hydroxy-pentyl)-2-imino-2,3-dihydro-imidazol-1-yl]-ethanone (ER 112787) (1 μM), completely inhibited it. The activated PAR1 involves the calcium-independent phospholipase-A_2 signaling pathway because two inhibitors of this cascade, bromoenol lactone (50 μM) and haloenol lactone suicide substrate (50 μM), block PAR1-thrombin-induced I_{NaP}. As a consequence of I_{NaP} activation, in guinea pig right ventricle papillary muscle, action potential duration (APD) were significantly increased by 20% and 15% under the respective action of 32 U/ml thrombin and 50 μM SFLLR-NH_2, and these increases in APD were prevented by 1 μM tetrodotoxin or markedly reduced by application of 1 μM SCH 203099 or ER 112787. Thrombin, through PAR1 activation, increases persistent component of the Na^+ current resulting in an uncontrolled sodium influx into the cardiomyocyte, which can contribute to cellular injuries observed during cardiac ischemia.

Thrombin is a serine protease released by thrombus with well-characterized roles in hemostasis, inflammation, and proliferative process. During cardiac ischemia reperfusion, thrombin is an important mediator of myocardial injury (Erlich et al., 2000). Indeed, thrombin can permeate vessels or endocardial barrier by extravasation and therefore can affect the first layers of cardiomyocytes. Thus, thrombin levels may be locally elevated at site of vascular injury and thrombus formation and reach an activity as high as 10 to 30 U/ml (Park et al., 1994). Then, thrombin has multiple cellular effects mediated by a family of G-protein-coupled protease-activated receptors (PARs), of which PAR1 is the prototype (Coughlin, 2000). PAR1 are expressed in human myocardium (Jiang et al., 1996) and activates a spectrum of biochemical signals leading to changes in contractile performance and alteration in gene expression (Glembotski et al., 1993), sarcomeric organization, and cardiomyocyte morphology (Sabri et al., 2002). As shown recently, theses phenomenons are clearly involved in human coronary atherosclerosis and can lead to endothelial dysfunction and vascular inflammation (Lavi et al., 2007). Thus, thrombin stimulates phosphoinositide hydrolysis, for instance by converting phosphatidylcho-

This work was partly supported by Agence Nationale de la Recherche ANR-05-PCOD-006–01. C.P. was a recipient of grants from the Fondation Lefoulon Delalande and Association Française contre les Myopathies.

C.Pinet and V.A. contributed equally to this study.

[1] Current affiliation: Centre National de la Recherche Scientifique UMR 6187, Institut de Physiologie et de Biologie Cellulaire, Université de Poitiers, Poitiers, France.

Article, publication date, and citation information can be found at http://molpharm.aspetjournals.org.
doi:10.1124/mol.107.043182.

ABBREVIATIONS: PAR, protease-activated receptor; HELSS, haloenol lactone suicide substrate; SCH 203099, N^3-cyclopropyl-7-((4-(1-methylethyl)phenyl)methyl)-7*H*-pyrrolo(3,2-*f*)quinazoline-1,3-diamine; HP, holding potential; AP, action potential; APD, action potential duration; TTX, tetrodotoxin; PLA_2, phospholipase A_2; LPC, lysophosphatidyl choline; BEL, bromoenol lactone; ER 112787, 1-(3,5-di-*tert*-butyl-4-hydroxy-phenyl)-2-[3-(3-ethyl-3-hydroxy-pentyl)-2-imino-2,3-dihydro-imidazol-1-yl]-ethanone.

line into lysophosphatidylcholine (LPC), via PLA_2 (Park et al., 1994; Sabri et al., 2000). Thrombin also activates the extracellular signal-regulated protein kinase (Sabri et al., 2002), facilitates rapid sodium current (Pinet et al., 2002), modulates calcium homeostasis (Steinberg et al., 1991, 2005), increases arrhythmias (Goldstein et al., 1994), and hastens recovery from an imposed acid load by activating Na^+-H^+ exchange (Avkiran and Haworth, 2003). Taken together, these signal events profoundly alter electrophysiological properties and contractile behavior and could induce cardiomyocyte toxicity during the myocardial ischemia-reperfusion injuries.

Increase in intracellular sodium during ischemia plays a key role in intracellular calcium overload, resulting in myocyte injuries. The involvement of thrombin-dependent activation of PAR1 in Na^+ entry during ischemia has never been assessed. In a previous study, we reported that thrombin can reversibly act as direct agonist on I_{Na}. The main consequences of this action were the shift toward hyperpolarizing potentials of the activation-voltage relationship, the large increase in peak I_{Na} amplitude, and the consequent increase in the window of sodium current; however, this effect was independent of PAR1 activation (Pinet et al., 2002). The present study examines whether PAR1 signaling in human cardiomyocytes is involved in the effect of thrombin on sodium current specially the persistent sodium current (I_{NaP}) (Haigney et al., 1994; Maltsev et al., 1998; Fedida et al., 2006; Noble and Noble, 2006; Saint, 2006). The main result was that thrombin, by binding to PAR1 receptor, activates I_{NaP}.

Materials and Methods

Heart Tissue Samples. Protocols for obtaining human cardiac tissue were in conformation with the principles outlined in the Declaration of Helsinki. We used a total of 62 specimens of human right atrial appendages that were obtained from hearts of patients (51–74 years old) undergoing heart surgery for coronary artery bypass graft or valve replacement. Seven percent of patients had received β-adrenergic receptor blockers, 38% had received calcium antagonists, 45% had received antiulcer drugs, 8% had received diuretics, and 22% had received antithrombotics. Treatments were usually stopped 24 h before operation. Patients with atrial dilation were avoided, and none had a history of supraventricular arrhythmias.

Cell Isolation. Human atrial myocytes were isolated enzymatically as described previously (Antoine et al., 1998). The same chunk procedure was used to isolate myocytes from the right ventricle of guinea pig hearts, except that elastase was omitted in the chunks predigestion bath. Only quiescent rod-shaped myocytes with clear cross-striations, sharp edges, and a well delineated cell membrane were chosen for experiments. Small myocytes were preferred to optimize spatial voltage-clamp.

Solutions and Drugs. For whole-cell current recordings, the intracellular pipette solution contained 5 mM NaCl, 130 mM CsCl, 2 mM $MgCl_2$, 1 mM $CaCl_2$, 15 mM EGTA, 10 mM HEPES, and 4 mM MgATP, pH adjusted to 7.2 with CsOH; the basal external solution contained 25 mM NaCl, 108.5 mM CsCl, 2.5 mM $CoCl_2$, 0.5 mM $CaCl_2$, 2.5 mM $MgCl_2$, 5 mM 4-aminopyridine, 10 mM HEPES, and 10 mM glucose, pH adjusted to 7.4 with CsOH. Hirudin (from leeches, ≈2000 U/mg) was from Roche (Mannheim, Germany). Haloenol lactone suicide substrate (HELSS) from TEBU France, was dissolved in dimethyl sulfoxide that did not exceed 0.05%. The PAR1 agonist ($SFLLR-NH_2$) and antagonist SCH 203099 were from the Division of Medicinal Chemistry IV (Centre de Recherche Pierre Fabre, Castres, France), α-thrombin (human plasma ≈ 1000 U/mg), and other chemicals were purchased from Sigma (St. Quentin Fallavier, France). Commercially available lyophilized thrombin is provided as a sodium salt. The addition of 32 U/ml thrombin to the basal perfusion medium containing 25 mM NaCl increases the Na^+ activity to 32.1 ± 0.3 mM (n = 10) (measured with a sodium ion-selective electrode). The control perfusion medium was therefore supplied with NaCl to keep the Na^+ activity equivalent.

Current Recordings. Ionic currents were recorded by the whole-cell patch-clamp technique with a patch-clamp amplifier (Axopatch 200B, Axon Instruments, Foster City, CA). Patch pipettes (Corning Kovar Sealing code 7052; World Precision Instruments, Sarasota, FL) had resistances of 0.5 to 2.0 MΩ. Currents were filtered at 20 kHz (−3 dB, eight-pole, low-pass Bessel filter) and digitized at 50 kHz (Digidata 1200; Molecular Devices, Sunnyvale, CA).

Cell membrane capacitance was 48.2 ± 2.6 pF (n = 67 cells, from 62 donors) for human atrial myocytes and 62.4 ± 7.5 pA/pF (n = 18, from 10 hearts) for guinea pig right ventricular myocytes. Series resistance was compensated at 80 to 95%, resulting in voltage errors of <3 mV. Leakage current was compensated for, whereas cell membrane capacitive current was not. Peak I_{Na} and I_{NaP} amplitudes were monitored according to a steady-state pulse protocol: a 1000-ms depolarizing test pulse to −30 mV from a HP of −100 mV at 0.2 Hz. It is noteworthy that the test pulse chosen was beyond the upper limit of the potential range inside which the sodium window current has been observed to increase under the direct effect of thrombin on sodium channel (Pinet et al., 2002). To avoid a putative overlap between PAR1-induced I_{NaP} and thrombin-increased sodium window current, experiments were also performed with test pulse to −10 mV. An equilibration period was allowed until peak I_{Na} reached steady state and remained stable without evidence of a leftward shift of the availability-voltage relationship (h_∞-V_m). This protocol was designed to detect any such shifts. After each sequence of five depolarizing pulses, HP was set to −140 mV. Consequently, during the stabilization period, when peak current amplitude was higher after a HP at −140 mV compared with −100 mV, the recording was discarded. Likewise, because thrombin has no effect on the h_∞-V_m relationship (Pinet et al., 2002), recordings showing an irreversible hyperpolarizing shift of h_∞-V_m after thrombin application were also discarded. The steady-state pulse protocol was applied in control, thrombin, or when other substances were tested and washed out. Experiments were carried out at room temperature (22–25°C).

Action Potential Recording. Male guinea pigs were anesthetized by intraperitoneal pentobarbital sodium injection, and their hearts were quickly removed. The investigation conforms with the *Guide for the Care and Use of Laboratory Animals* published by the U.S. National Institutes of Health (NIH Publication no. 85-23, revised 1996). A total of 21 hearts were used for the AP study. Papillary muscles were dissected from the right ventricle and superfused (4–6 ml/min) with the Krebs' solution maintained at 36.0 ± 0.5°C in a 5-ml tissue bath. The Krebs' solution was oxygenated with 95% O_2/5% CO_2 and had the following composition: 113.1 mM NaCl, 4.6 mM KCl, 2.45 mM $MgCl_2$, 3.5 mM NaH_2PO_4, 21.9 mM $NaHCO_3$, and 5 mM glucose, pH 7.4. Action potentials (AP) were recorded by conventional "floating" glass microelectrodes (5–20 MΩ) filled with 3 M KCl and were coupled to a high-input impedance preamplifier (VF 102; Biologic, Echirolles, France). The preparations were electrically stimulated (Pulsar BP; FHC, Bowdoin, ME) with 1-ms pulses at 1.5 times the threshold voltage through a bipolar Ag-electrode. APs were displayed on a dual-beam oscilloscope (TDS 2012; Tektronics, Heerenveen, The Netherlands) and simultaneously digitized and analyzed with interactive software (NOTOCORD-hem 3.4; Notocord Systems, Croissy Sur Seine, France). The preparations were allowed to equilibrate for at least 1 h at a stimulation rate of 1 Hz. A single impalement was maintained throughout control and compound superfusion periods. AP parameters measured were maximum upstroke velocity [$(dV/dt)_{max}$], amplitude, resting membrane potential, and action potential duration (APD) at 50 and 90% repolarization levels (APD_{50} and APD_{90}, respectively).

Data Analysis and Statistics. As much as possible, depending on the experimental protocol performed, only the TTX-inhibited PAR1-induced I_{NaP} was taken into account and determined by sub-

tracting the current obtained under concomitant application of TTX and thrombin or SFLLR-NH_2 from that previously recorded under thrombin alone. The amplitude of TTX-blocked thrombin-induced I_{NaP} was the mean current calculated from 80 to 180 ms after the beginning of the depolarization (Valdivia et al., 2002). Peak I_{Na} amplitude was measured with respect to current amplitude at the end of the test pulse. Data are expressed as means ± S.E.M. of n determinations or myocytes. Statistical analysis were performed by using paired or unpaired Student's t test or analysis of variance, as appropriate, and the null hypothesis was rejected at the 0.05 level; *, $p < 0.05$; **, $p < 0.01$; and ***, $p < 0.001$.

Results

Thrombin Application Induced a Persistent Sodium Current Different from the Thrombin-Increased Sodium Window Current. To be beyond the upper limit of the range of membrane potential (from −85 to −40 mV) in which sodium window current occurs, a test pulse to −30 mV was used to elicit I_{Na} (Pinet et al., 2002). Local perfusion of 32 U/ml thrombin on freshly isolated human atrial myocytes caused the already described marked increase in peak of I_{Na} (Fig. 1 A), which occurred rapidly (Fig. 1D) and was shown to be completely independent of the activation of PAR1 receptors (Pinet et al., 2002). In addition to this effect on peak I_{Na}, after a longer time of application, over 6 min, thrombin induced very slowly inactivating or persistent TTX-blocked sodium current (Fig. 1, B and D), termed I_{NaP}. Although the increase in peak I_{Na} was observed in all tested cells, the induction of I_{NaP} was observed in 51 of 67 cells, most proba-

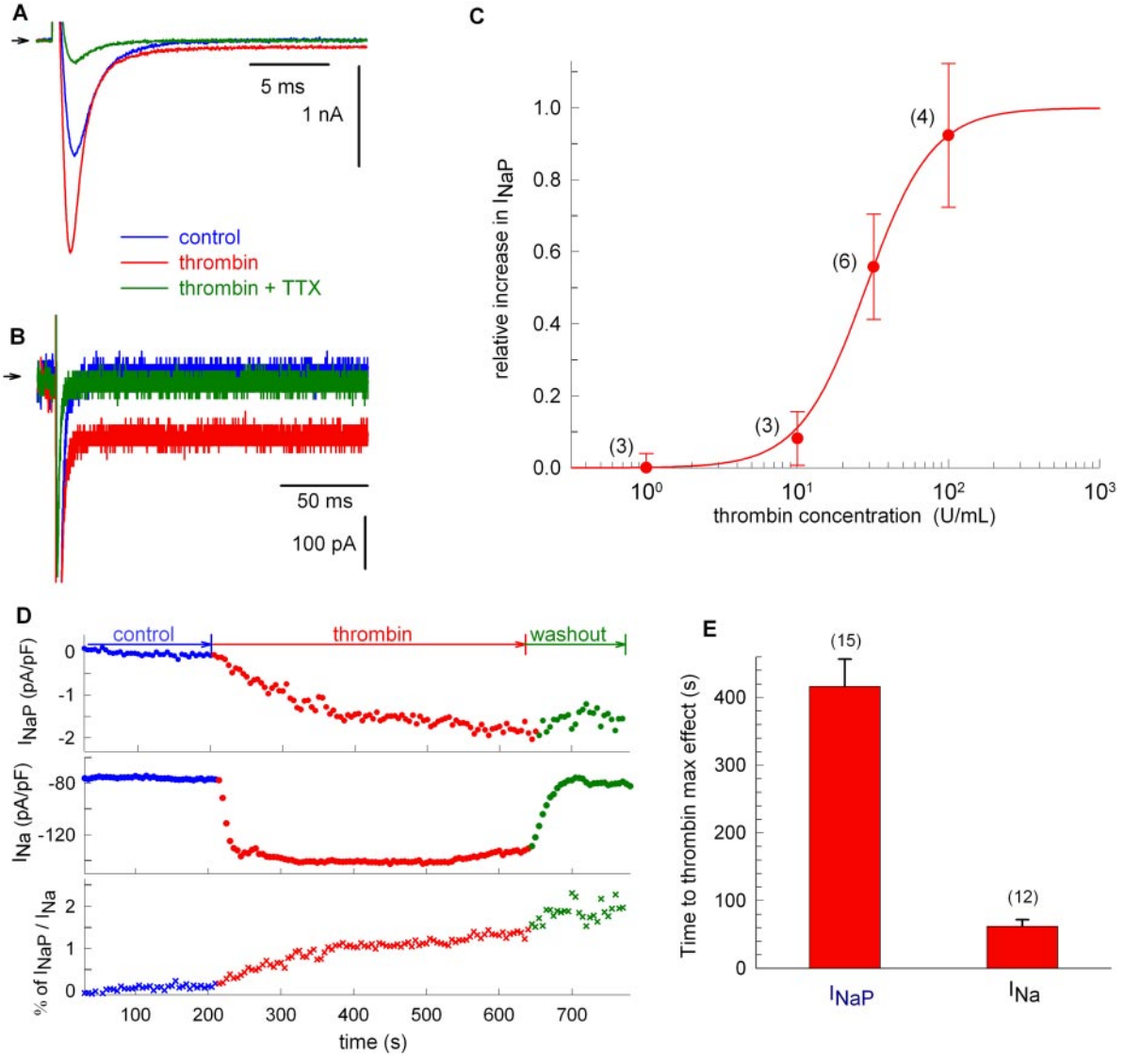

Fig. 1. Rapid sodium current was modified after thrombin application to human atrial myocytes. A shows that thrombin (32 U/ml) was able to increase the TTX-blocked fast sodium current I_{Na}, as described previously. In B, the vertical scale shows a higher gain than in A, and the time base is slowed to demonstrate the effect of thrombin on the noninactivating persistent component of the current (I_{NaP}), which was blocked by 50 μM TTX. Arrows indicate zero current level. C, concentration-response curve for thrombin-induced I_{NaP}. Normalized mean increase in I_{NaP} amplitude is reported against thrombin activity. Each point represents the mean ± S.E.M. of n measurements indicated. Data points were fitted by the equation $Y/Y_{max} = 1/[1 + (EC_{50}/\text{thrombin activity})^{n_H}]$. Y_{max} (maximum mean induced-I_{NaP}), EC_{50} (activity inducing half-maximal effect), and Hill parameter n_H were, 3.98 pA/pF, 28.4 U/ml, and 1.98 for I_{NaP}, respectively. D, kinetic of the effect of thrombin on I_{NaP} and on peak I_{Na}. Time courses of I_{NaP} (top) and of peak I_{Na} (middle) densities, and percentage of induced I_{NaP} over peak I_{Na} (bottom), under conditions indicated by horizontal bars. Currents were elicited by depolarization from HP = −140 to −30 mV. E, bar graphs correspond to the time necessary to obtain the thrombin maximal effect on the two currents; the number of measurements is in parentheses.

bly as a consequence of the lost and/or damage caused to PAR1 receptors by the enzymatic procedure used for cell dissociation. Thrombin (32 U/ml) increased peak I_{Na} from -118.9 ± 12.6 to -191.7 ± 20.8 pA/pF ($n = 23$; $p < 0.001$, paired t test) and induced I_{NaP} in a concentration-dependent manner (Fig. 1C). At this concentration of thrombin, maximum increase in I_{NaP} was 1.8% of control peak I_{Na}. The density of I_{NaP} was -0.02 ± 0.01 pA/pF, $n = 3$, with 1 U/ml thrombin, -0.50 ± 0.02 pA/pF, $n = 3$, with 10 U/ml thrombin, -2.23 ± 0.54 pA/pF, $n = 6$, with 32 U/ml thrombin, and -3.69 ± 0.82 pA/pF, $n = 4$, with 100 U/ml thrombin. Estimated-maximal density of I_{NaP} was -3.98 pA/pF, and the apparent EC_{50} and the Hill coefficient were 28.4 U/ml and 1.98, respectively. This concentration-response relationship exhibits clear differences compared with the reported concentration-response of the effect on peak I_{Na} (Pinet et al., 2002) where EC_{50} and Hill coefficient were 91 U/ml and 0.75, respectively. Thrombin-induced I_{NaP} was not a residual current resulting from the thrombin-enhanced window sodium current (Pinet et al., 2002), because the increase in I_{NaP}, with 32 U/ml thrombin, was observed with test pulses to -10 mV, a membrane potential at which the window current could not be activated (I_{NaP} density was -1.71 ± 0.83 pA/pF; $n = 5$). These two distinct effects of thrombin on sodium current (increase in peak I_{Na} and in I_{NaP}) were suppressed by 50 μM TTX, a specific sodium channel blocker (Fig. 1, A and B). It is noteworthy that the difference in kinetics of thrombin effect on peak I_{Na} compared with the onset of I_{NaP} (Fig. 1D) and that the time to reach maximum thrombin effects was much longer for I_{NaP} (416.0 $\pm$ 40.4 s, $n = 15$) than for peak I_{Na} (61.7 $\pm$ 10.1 s, $n = 12$; Fig. 1E), suggesting distinct underlying mechanisms. This is also supported by the observation that after washout of thrombin, the amplitude of peak I_{Na} returned to the basal (Pinet et al., 2002) but not that of I_{NaP} (Fig. 1D), in accordance with the irreversibility of the cleavage of PAR1 by thrombin. The below of Fig. 1D exemplifies the prominence of thrombin effect on I_{NaP} over the effect on peak I_{Na}, when the latter effect wore out.

Involvement of the PAR1 in Thrombin-Induced I_{NaP}. To test further for the requirement of protease activity of thrombin in the activation of I_{NaP}, we investigated the effect of hirudin, a direct protease inhibitor of thrombin. The induction of I_{NaP} by 32 U/ml thrombin was markedly reduced in presence of 320 U/ml hirudin (Fig. 2B–D); I_{NaP} density was, under thrombin, -2.27 ± 0.51 pA/pF ($n = 8$) versus -0.43 ± 0.19 pA/pF under thrombin in presence of hirudin ($n = 9$; $p < 0.001$), whereas the effect of thrombin on peak I_{Na} was unchanged (Fig. 2, A and C). This result confirms that the protease activity of thrombin was necessary to activate I_{NaP}, probably through the cleavage of still undefined target proteins. Among the proteins cleaved by thrombin, the most likely target protein is the well known PAR1 receptor. To study the involvement of this receptor, the selective PAR1-antagonist SCH 203099 (Ahn and Chackalamannil, 2001) has been used. After human atrial cell preincubation with 10 μM SCH 203099 for at least 15 min, thrombin failed to induce I_{NaP} [Fig. 3, B–D; -0.30 ± 0.07 pA/pF ($n = 14$) versus -2.27 ± 0.51 pA/pF, $n = 8$ in absence of SCH 203099 ($p < 0.001$)], whereas the thrombin effect on peak I_{Na} was unaffected [Fig. 3, A and C; from -103.7 ± 14.1 pA/pF under SCH 203099 to -158.4 ± 21.6 pA/pF ($n = 14$) after addition of 32 U/ml thrombin ($p < 0.001$)]. These results suggest that PAR1 activation constitutes a key mechanism for the thrombin-induced I_{NaP}. Then, the ability of the PAR1 agonist peptide SFLLR-NH_2 to putatively mimic the role of thrombin in induction of I_{NaP} via PAR1 was tested (Fig. 4). SFLLR-NH_2 stimulated I_{NaP} [mean increased: -1.46 ± 0.63 pA/pF, $n = 5$, $p < 0.05$ versus control (Fig. 4, B and C)], exhibiting a fair reversibility upon washout (Fig. 4, B and D) but failed to increase peak I_{Na} (Fig. 4, A and D). Taken together, the present results demonstrate that the thrombin-induced I_{NaP} is mediated by PAR1 activation.

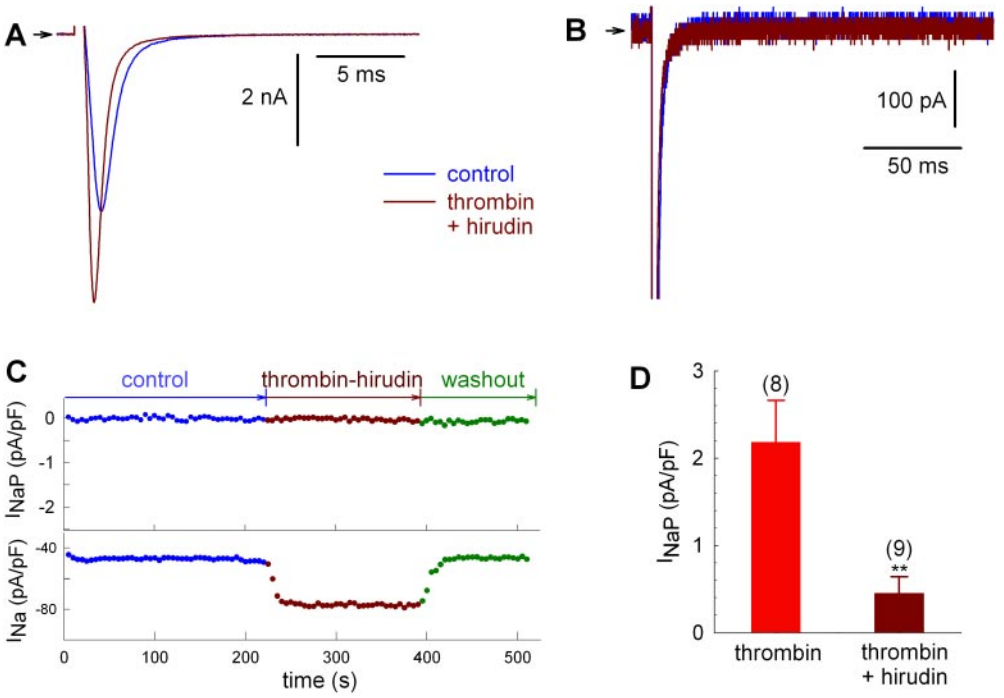

Fig. 2. The effect of hirudin, a direct inhibitor of the protease activity of thrombin, was tested on thrombin-induced I_{NaP}. Typical current recordings (represented as in Fig. 1) showing that coapplication of hirudin (320 mM) left unchanged the increase in peak I_{Na} by thrombin (32 U/ml) (A) but prevents the thrombin-induced I_{NaP} (B). C, kinetic comparisons of the action of thrombin in presence of hirudin on I_{NaP} and on peak I_{Na}. Time courses of I_{NaP} (upper trace) and of peak I_{Na} (lower trace) densities, under conditions indicated by horizontal bars. Currents were elicited as described in the legend to Fig. 1. D, bar graphs confirm that hirudin prevented the induction of I_{NaP} by thrombin.

Involvement of Ca^{2+}-Independent Phospholipase-A_2 Pathways after PAR1 Activation. PAR1 is a member of the G-protein-coupled receptor family; therefore, its activation stimulates numerous intracellular signaling pathways (Coughlin, 2000). Several studies have reported that in cardiomyocytes, thrombin stimulates the Ca^{2+}-independent phospholipase A_2 (PLA_2) via PAR1, which produced an intracellular lysophosphatidyl choline (LPC) accumulation (Park et al., 1994; Yan et al., 1995). Therefore, two inhibitors of PLA_2 [bromoenol lactone (BEL) and haloenol lactone suicide substrate (HELSS)] were used to investigate whether PLA_2 activity is involved in the enhancement of I_{NaP}, induced by PAR1 stimulation. After cell incubation with BEL for at least 30 min, thrombin had its usual effect on peak I_{Na} (Fig. 5A) but failed to stimulate I_{NaP} (Fig. 5B, -0.22 ± 0.11 pA/pF, $n = 5$ versus -2.27 ± 0.51 pA/pF, $n = 8$, in the absence of BEL; $p < 0.01$). A similar result was obtained with HELSS (Fig. 5C). The density of I_{NaP} activated in presence of thrombin and HELSS was -0.39 ± 0.14 pA/pF, $n = 5$ ($p < 0.01$). These results indicate that the PAR1-induced I_{NaP} required the activation of Ca^{2+}-independent PLA_2.

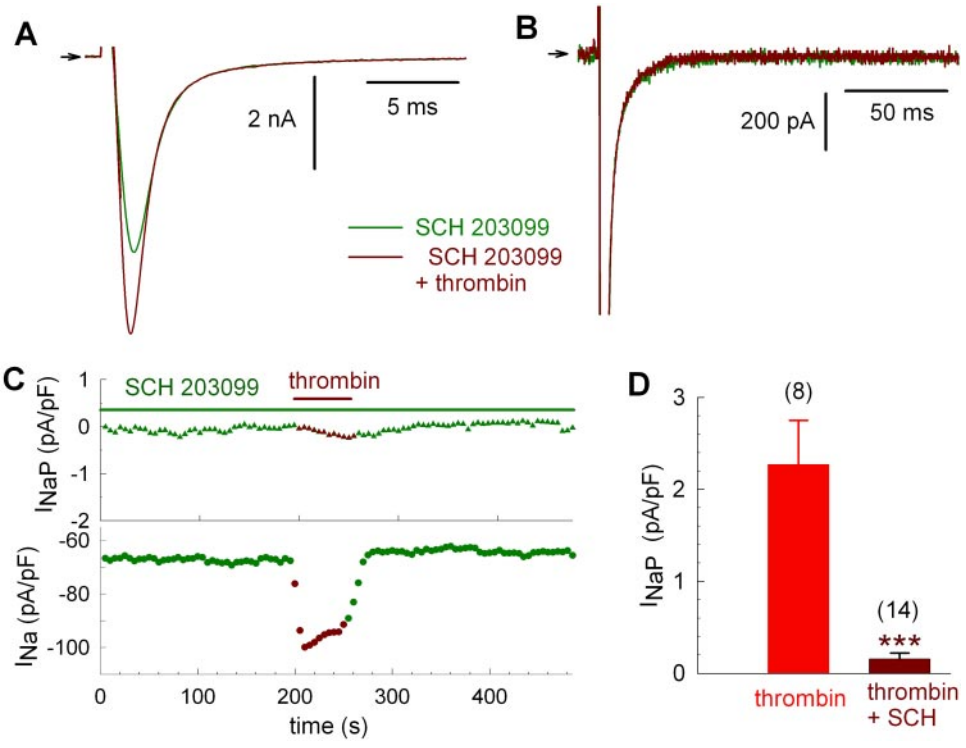

Fig. 3. Because the induction of I_{NaP} depended on the protease activity of thrombin, the involvement of the protease-activated-receptor 1 (PAR1) was tested using the PAR1 antagonist SCH 203099. A, current traces showing that SCH 203099 does not prevent the increase in peak I_{Na} by thrombin, whereas it blocks the thrombin-induced I_{NaP} (B). C, time courses of I_{NaP} and I_{Na} densities, under conditions indicated by horizontal bars. D, bar graphs summarize the effect of SCH 203099 versus thrombin on I_{NaP}. Thrombin was used at 32 U/ml and SCH 203099 at 10 μM.

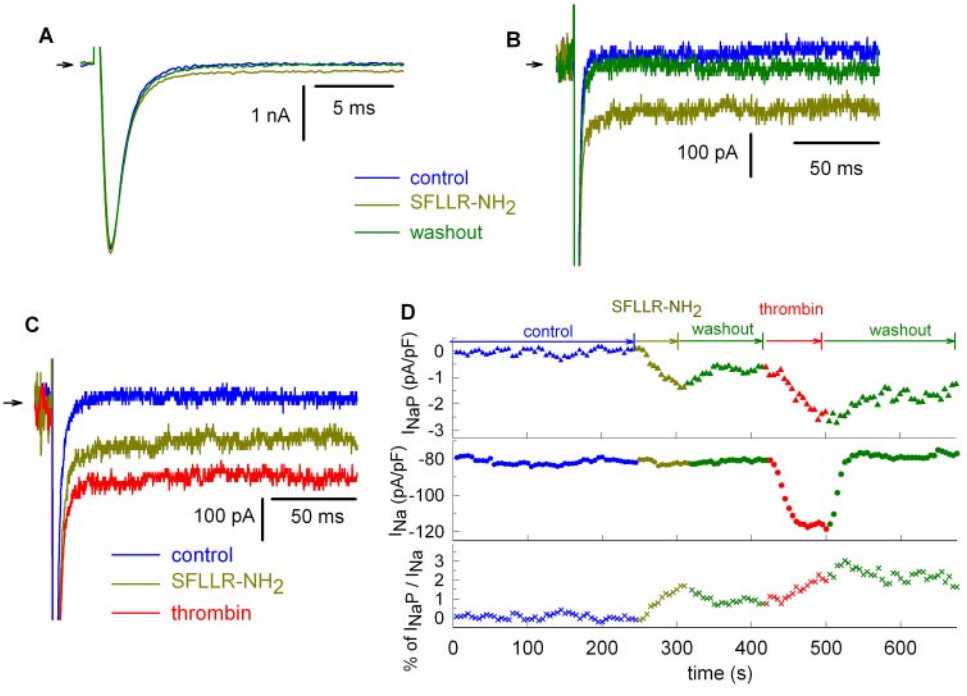

Fig. 4. SFLLR-NH_2, a synthetic PAR1 agonist peptide, was able to reproduce the potent induction of I_{NaP} by thrombin but not the increase in peak I_{Na}. Typical current traces of I_{Na} (A) showing activation of I_{NaP} and that peak I_{Na} remained unchanged under SFLLR-NH_2. B, the corresponding traces with different amplitude- and time-scales on right hand. C and D, the effect of SFLLR-NH_2 on I_{Na} was compared with thrombin-activation of I_{NaP}. In C, typical traces of I_{NaP} were obtained under control, SFLLR-NH_2 and thrombin conditions. In D, comparison of I_{NaP} (top) and I_{Na} (middle) time courses, and percentage of I_{NaP} over I_{Na} (bottom), under conditions indicated by horizontal bars, showing the activation of I_{NaP} by SFLLR-NH_2, followed by its partial reversion upon washout, and the usual effects of thrombin. SFLLR-NH_2 was used at 50 μM and thrombin at 32 U/ml.

Thrombin and PAR1 Agonist Peptide SFLLR-NH$_2$ Increased Action Potential Duration. To examine the consequence of activation of I_{NaP} by thrombin and PAR1 agonist peptide SFLLR-NH$_2$ on cardiac tissue electrical activity, we recorded action potentials in right ventricle papillary muscle from guinea pigs. We used the classic microelectrode technique, which allows a stable and reliable AP recording during prolonged period as required for the study of the delayed effect of thrombin on I_{NaP}. We first checked that, in this species and in ventricular cells, thrombin also activates I_{NaP} by performing patch-clamp experiments in isolated guinea pig ventricular myocytes. Test pulses to −10 mV from a holding potential of −80 mV were used to elicit current. Immediate application of thrombin (32 U/ml) increased peak I_{Na} (Fig. 6A, a and b) from −112.6 ± 11.5 to −166.9 ± 16.4 pA/pF, n = 11 ($p < 0.001$; paired t test), blocked by application of 50 μM TTX. Moreover, after 7 min of application, thrombin induced a TTX-sensitive I_{NaP} of −2.91 ± 1.1 pA/pF, n = 9 (Fig. 6A, b and d). The increase in I_{NaP} was 0.026% of control peak I_{Na}. This effect was blocked by the PAR1 antagonist ER 112787 (Barry et al., 2006; Chackalamannil and Xia, 2006) (Fig. 6B). After myocyte-preincubation with 1 μM ER 112787 for at least 5 min, thrombin did not induced I_{NaP} [Fig. 6B, b, c, and d; −0.076 ± 0.05 pA/pF (n = 5) versus −2.91 ± 0.68 pA/pF, in absence of drug, n = 9; $p < 0.001$], whereas the effect of thrombin on peak I_{Na} was unaffected (Fig. 6A, a and c; −87.3 ± 6.1 pA/pF, n = 5, under ER 112787 to −123.4 ± 10.3 pA/pF, n = 9, after addition of thrombin; $p < 0.05$).

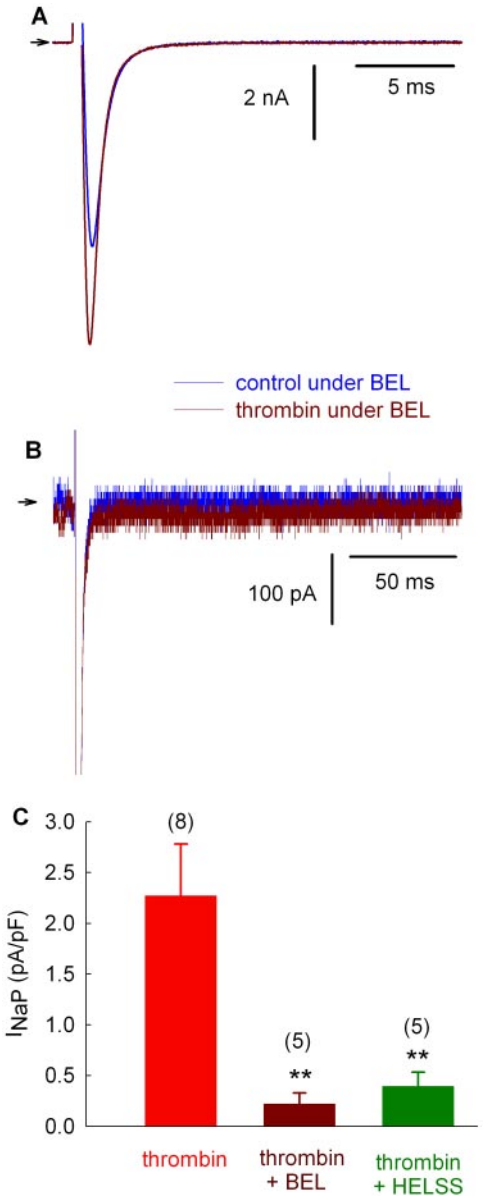

Fig. 5. Thrombin-induced I_{NaP} requires activation of Ca^{2+}-independent phospholipase A_2. Effects of BEL, a PLA_2 inhibitor, upon thrombin-increased peak I_{Na} (A) and thrombin-induced I_{NaP} (B). A, sample current traces showing no effect of BEL on thrombin-increased peak I_{Na}. B, the corresponding traces with different amplitude- and time-scales demonstrating that the presence of BEL prevented the induction of I_{NaP}. Cell was previously preincubated with 50 μM BEL for 30 min. C, bar graphs summarizing the inhibition of thrombin-induced I_{NaP} after BEL incubation and HELSS application. Thrombin was used at 32 U/ml and HELSS at 10 μM.

Figure 7A, a, shows the effects of thrombin (32 U/ml) and SFLLR-NH$_2$ on action potentials recorded from right papillary ventricle. After a 10-min application, thrombin and SFLLR-NH$_2$ significantly increased APD measured at 50 and 90% of repolarization (Fig. 7A and Table 1). At these two levels of repolarization, the increases in APD were 15.3 and 12.9%, respectively, for thrombin and 12.4 and 12.1% for SFLLR-NH$_2$ (Table 1). The increases in APD were barely reversible (Table 1). It is noteworthy that in presence of TTX (1 μM), applications of thrombin (32 U/ml) or SFLLR-NH$_2$ (100 μM) failed to increase the action potential duration (Fig. 7A, b, and Table 2). We used a low concentration of TTX to minimize the consequences of the inhibition of peak I_{Na} on AP upstroke.

To investigate the involvement of PAR1 on thrombin- and SFLLR-NH$_2$-induced APD lengthening, two selective PAR1 antagonists, SCH 203099 and ER 112787, were then evaluated. Figure 7B, a and b, show that both SCH 203099 and ER 112787, in a concentration-dependent manner, reduced the thrombin- and SFLLR-NH$_2$-induced APD prolongations. Thus, SCH 203099 (10 μM) and ER 112787 (1 μM) both fully blocked the APD prolongation induced by 100 μM SFLLR-NH$_2$ (Fig. 7B), a result that was in complete agreement with the potency of this antagonist against PAR1 (Chackalamannil and Xia, 2006). Taken together, these results indicated that stimulation of the inward persistent Na^+ current by protease-activated receptors after PAR1 activation can modify the AP duration.

Discussion

The present results demonstrate for the first time that thrombin induces a PAR1-mediated persistent sodium current component, I_{NaP}, in cardiomyocytes. Because thrombin is a serine protease formed at the site of coronary vascular wall injury, this effect on Na current might have important consequences in the setting of myocardial ischemia.

Involvement of PAR1 Signaling Pathway in the Thrombin Effect on I_{NaP}. The conclusion that thrombin enhances I_{NaP} through the proteolytic cleavage of PAR1 is supported by the findings that this thrombin effect on current is mimicked by the PAR1 agonist peptide SFLLR-NH$_2$ and is fully blocked by the PAR1 antagonists, SCH 203099 and ER 112787 (Ahn and Chackalamannil, 2001). Cleavage of the amino-terminal PAR1 exodomain unmasks a tethered

ligand that binds the receptor body to trigger intracellular signaling. Consequently, PAR1 is irreversibly activated by this proteolytic cleavage, contributing to keep on its signal-transducing capability. This could explain the low reversibility of the thrombin effect on I_{NaP} upon washout (see Fig. 1). This was not the case for SFLLR-NH_2 (see Fig. 4), an exog-

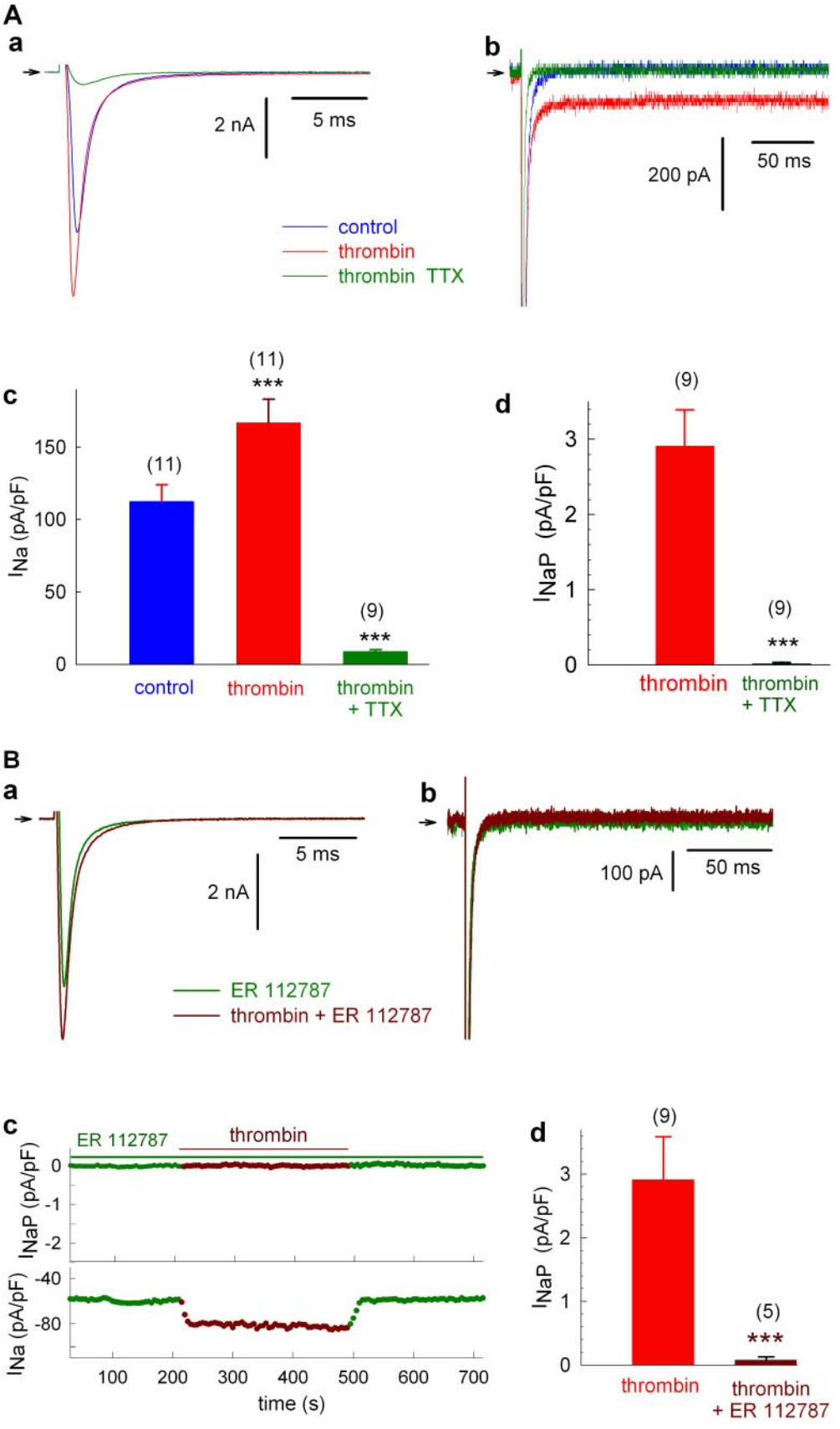

Fig. 6. Guinea pig ventricular myocytes also exhibited a thrombin-increased I_{Na} and a thrombin-induced I_{NaP}. A, a, shows that thrombin (32 U/ml) was able to increase the TTX-blocked fast sodium current I_{Na}. b, the corresponding traces with different amplitude- and time-scales showing the TTX-blocked, thrombin-induced-I_{NaP} recorded after 7-min application of thrombin (32 U/ml). TTX was used at 50 μM. c and d, bar graphs summarizing the effects of thrombin and TTX on I_{Na} and I_{NaP}. B, with this cell type, another PAR1-antagonist, ER 112787, has been tested. a, current traces showing that ER 112787 did not prevent the increase in peak I_{Na} by thrombin, whereas it blocked the thrombin-induced I_{NaP} (b). c, time courses of I_{NaP} and I_{Na} densities, under conditions indicated by horizontal bars. d, bar graphs summarize the effect of ER 112787 versus thrombin on I_{NaP}. Thrombin was used at 32 U/ml and ER 112787 at 1 μM.

enous peptide that does not cleave the PAR1 and that exhibited an effect more sensitive to washout. Another evidence that thrombin effect on I_{NaP} is mediated by PAR1 signaling pathways is provided by the observation that this effect is suppressed by the inhibition of PLA$_2$ by BEL and HELSS. There are previous studies showing that the increase in intracellular LPC levels plays an important role in the thrombin effect (Undrovinas et al., 1992; Park et al., 1994; Yan et al., 1995). For instance, the cleavage of PAR1 by thrombin stimulates the amphipathic lipids catabolism leading to an accumulation of LPC in the intracellular medium (Undrovinas et al., 1992; Park et al., 1994). However, the precise level of the signaling pathway at which PLA$_2$ inhibitors were able to inhibit thrombin-induced I_{NaP} remains to be clarified.

Nature of the I_{NaP} Current. The intracellular accumulation of LPC could mediate the effect of thrombin on I_{NaP}. The LPC is well known to maintain sodium channel in burst-

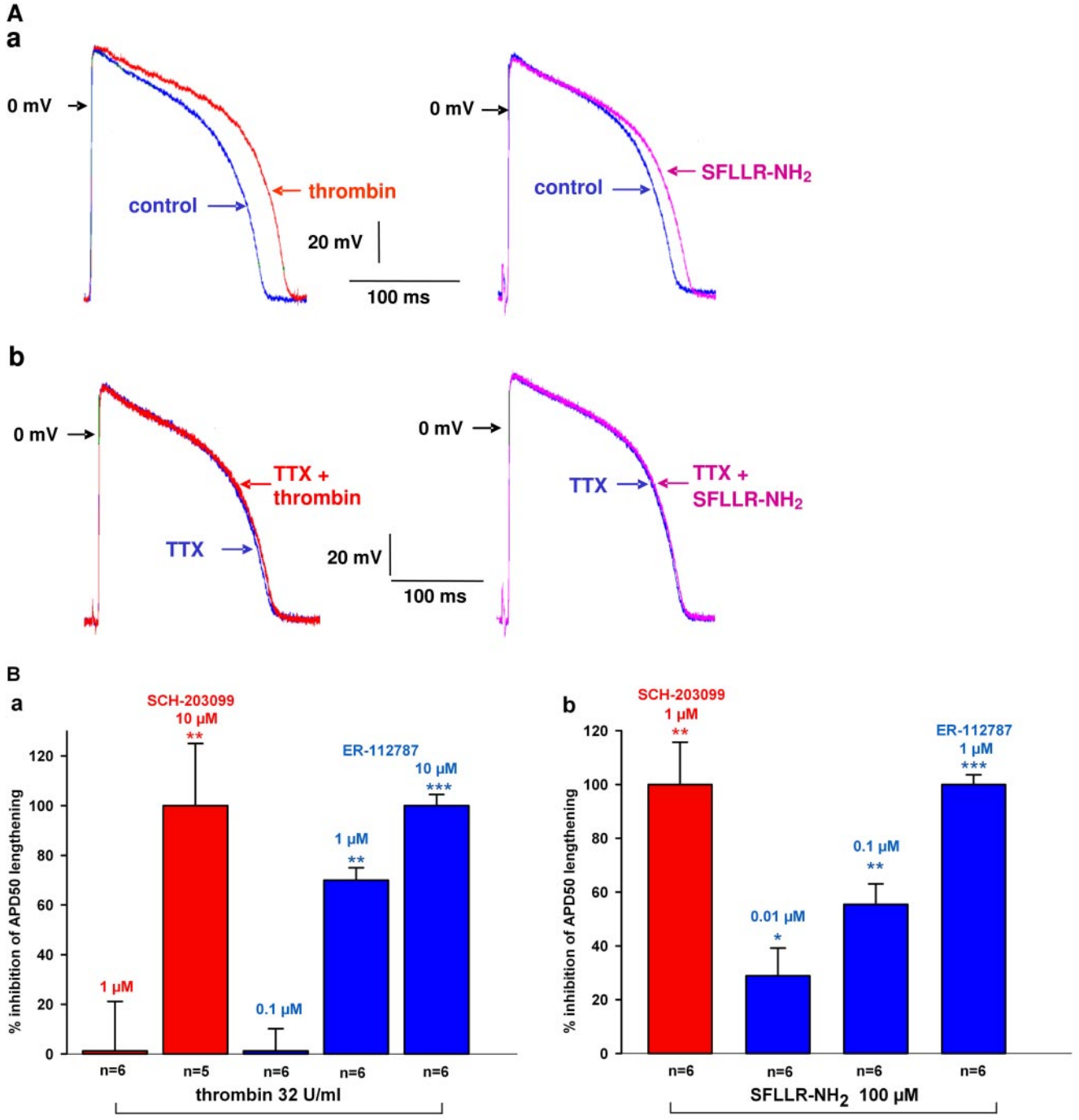

Fig. 7. A, direct applications of thrombin or of the synthetic PAR1 agonist peptide SFLLR-NH$_2$ prolonged the action potential duration (a), prolongations prevented in presence of TTX (b). Action potentials were recorded from guinea pig right ventricular papillary muscles before and 15 min after the applications of thrombin (32 U/ml) or SFLLR-NH$_2$ (100 μM) (a) and when those applications were performed in presence of 1 μM TTX (b). Arrows indicate zero potential level. B, effects of two selective PAR1 antagonists, SCH 203099 and ER 112787, on thrombin- and SFLLR-induced APD-lengthening (a and b). Bar graphs showing the concentration-responses inhibition effect of SCH 203099 and ER 112787 on thrombin- and SFLLR-lengthened APD of action potentials recorded from guinea pig right ventricular papillary muscles.

ing activity, thus giving rise to noninactivating sodium current (Undrovinas et al., 1992). The exact nature of this noninactivating sodium current is not yet fully elucidated. There is evidence that this persistent component of sodium current, I_{NaP}, could be generated by a small fraction of the "normal" transient-mode sodium channel population, that undergoes burst or/and late scattered mode(s). Such modes have been recently described by Maltsev and Undrovinas (2006) for the persistent Na^+ current in human ventricular myocytes. Thus, thrombin could favor this bursting activity of voltage-gated sodium channels, by cleaving PAR1 and stimulating the conversion of phosphatidylcholine into LPC, which, via PLA_2 (Park et al., 1994; Sabri et al., 2000), increases intracellular LPC (Undrovinas et al., 1992; Park et al., 1994). In a previous study, we reported that thrombin stimulates the peak I_{Na} and the sodium-window current. However, this effect, which is fast and fully reversible, is not mediated by PAR1 (Pinet et al., 2002) as further demonstrated in the present study. Moreover, thrombin was able to induce I_{NaP} at membrane potentials as high as −10 mV, which is clearly not in membrane potential range of window current (from −85 to −40 mV). Finally, there are clear differences between the concentration-response curves of the effect of thrombin on peak I_{Na} (Pinet et al., 2002) and on I_{NaP}. One hypothesis currently tested concerning the direct effect of thrombin on peak I_{Na} is the involvement of a β-subunit (Herfst et al., 2003). The majority of Na^+ channels in the heart correspond to the expression of the TTX-resistant $Na_V1.5$ isoform, and this is the case for human atrial myocytes (Makielski et al., 2003). However, it cannot be excluded that thrombin-PAR1 activation targets another population of sodium channels (Brette and Orchard, 2006). The effect of thrombin on I_{NaP} that develops slowly is likely to have more significant consequences on cardiac myocyte.

Pathophysiological Consequences of the Activation by Thrombin of I_{NaP}. Both persistent and window sodium current are known to participate to action potential duration. Although the window sodium current, which activates in a restricted membrane potential range from −85 to −40 mV, is involved in the late phase of repolarization and in the control of resting membrane potential (Pinet et al., 2002), I_{NaP}, activated from −10 mV, is found to contribute to the regulation of the early phase of APD (Kiyosue and Arita, 1989; Maltsev et al., 1998; Sakmann et al., 2000; Fedida et al., 2006; Noble and Noble, 2006; Wu et al., 2006). It has been previously reported that blocking the I_{NaP} with TTX caused a 10 to 20% decrease of APD, although this current is of very small density in control condition (Kiyosue and Arita, 1989; Maltsev et al., 1998; Sakmann et al., 2000). Therefore, the progressive several-fold increase in I_{NaP} by thrombin is likely to have a significant effect on APD, whereas, despite a fast increase in peak I_{Na} (Fig. 1), thrombin is devoid of significant effect on $(dV/dt)_{max}$. Indeed, thrombin and SFLLR markedly increased the duration of action potentials of guinea pig papillary muscle. This effect of thrombin or SFLLR-NH_2 on AP duration can be largely explained by an increase of I_{NaP}, because it was abolished by TTX. However, it cannot be excluded that the thrombin/PAR1 pathway can affect other ionic currents indirectly via changes in $[Na]_i$ and $[Ca]_i$. Previous studies have shown that thrombin lengthens APD and increases cesium-induced early afterdepolarizations and pro-arrhythmic events in canine Purkinje fibers (Steinberg et al., 1991) and in intact adult rat hearts during early reperfusion (Jacobsen et al., 1996; Woodcock et al., 1998). It has been shown

TABLE 1

Effects of thrombin and SFLLR on action potential parameters

Guinea pig right ventricular papillary muscle action potential parameters determined in absence of TTX. Parameters were determined at least 15 min after the applications of thrombin or SFLLR-NH_2. Data are means ± S.E.M.

	n	RP	APD_{50}	APD_{90}	$(dV/dt)_{max}$
		mV	*ms*	*ms*	*V/s*
Thrombin, 32 U/ml					
Control	6	−91.6 ± 0.9	134.5 ± 10.3	159.5 ± 11.2	244 ± 29
Thrombin	6	−90.2 ± 0.6	155.1 ± 14.5*	180.2 ± 16.3*	252 ± 33
Washout	4	−91.9 ± 0.4	143.7 ± 16.7	167.6 ± 18.1	264 ± 45
SFLLR-NH_2, 100 μM					
Control	6	−92.3 ± 0.4	125.2 ± 19.5	153.7 ± 22.7	219 ± 12
SFLLR-NH_2	6	−89.4 ± 0.9	140.7 ± 21.8*	172.4 ± 27.1*	213 ± 16
Washout	4	−90.5 ± 0.6	150.3 ± 25.4	181.6 ± 31.6	225 ± 13

RP, resting membrane potential; APD_{50} and APD_{90}, action potential duration measured respectively at 50 and 90% of repolarization; $(dV/dt)_{max}$, maximum upstroke velocity.

* $p < 0.05$.

TABLE 2

Effects of thrombin and SFLLR on action potential parameters

Guinea pig right ventricular papillary muscle action potential parameters determined in presence of TTX. In both procedures, parameters were determined at least 15 min after the applications of thrombin or SFLLR-NH_2. Data are means ± S.E.M.

	n	RP	APD_{50}	APD_{90}	$(dV/dt)_{max}$
		mV	*ms*	*ms*	*V/s*
Thrombin, 32 U/ml					
TTX	5	−92.1 ± 1.4	162.9 ± 7.6	195.7 ± 5.5	205 ± 19
TTX & Thrombin	5	−90.9 ± 1.3	163.9 ± 11.3	195.1 ± 10.2	206 ± 28
SFLLR-NH_2, 100 μM					
TTX	4	−91.6 ± 1.1	161.4 ± 16.4	192.9 ± 16.1	165 ± 8
TTX & SFLLR-NH_2	4	−92.1 ± 0.8	166.7 ± 16.1	198.4 ± 16.3	158 ± 10

RP, resting membrane potential; APD_{50} and APD_{90}, action potential duration measured respectively at 50 and 90% of repolarization; $(dV/dt)_{max}$, maximum upstroke velocity.

also that suppression of the late sodium current can suppress EADs of myocytes isolated from failing hearts (Maltsev et al., 1998; Undrovinas et al., 2002; Valdivia et al., 2005; Fedida et al., 2006). Thus, blocking I_{NaP} by inhibiting PAR1 – PLA_2 pathway may be a new pharmacological target to reduce thrombin-induced arrhythmic activity.

Yan et al. (1995) have demonstrated that activation of PAR1 by SFLLR-NH_2 peptide induced a rapid and dramatic elevation in $[Na^+]_i$, which was associated with a concomitant increase in LPC content in isolated, blood-perfused rabbit hearts in response to ischemia (Lavi et al., 2007). The increase in $[Na^+]_i$ could contribute to myocyte injury during ischemia as the result of intracellular calcium overload and the activation of Ca^{2+}-dependent signaling cascades. This hypothesis is supported by the recent finding of the cardioprotective effects of the late sodium current inhibitor ranolazine (Belardinelli et al., 2006). Moreover, in in vivo and in vitro studies, Strande et al. (2007) have shown that a preventive and a curative treatments with a selective PAR1 antagonist reduced the infarct size and increased ventricular function recovery after ischemia reperfusion in an isolated heart model. It remains to determine whether the increase in $[Na^+]_i$ induced by SFLLR-NH_2 or by thrombin during ischemia is mediated by the activation of I_{NaP}.

In conclusion, this study describes a new regulatory mechanism of sodium current involving PAR1-PLA_2 signaling pathway, which could be evoked by thrombin during cardiac ischemia and thrombus formation (Haigney et al., 1994; Maltsev et al., 1998). Selective antagonists of PAR1 receptor, which are very efficient to suppress this effect of thrombin, might represent a novel cardioprotective strategy in the clinical setting of myocardial ischemia and reperfusion (Strande et al., 2007).

Acknowledgments

We are grateful to Dr. Elise Balse for careful reading of the manuscript.

References

Ahn H and Chackalamannil S (2001) Nonpeptide thrombin receptors antagonists. *Drugs Future* **26:**1065–1085.

Antoine S, Lefevre T, Coraboeuf E, Nottin R, and Coulombe A (1998) B-type Ca^{2+} channels activated by chlorpromazine and free radicals in membrane of human atrial myocytes. *J Mol Cell Cardiol* **30:**2623–2636.

Avkiran M and Haworth RS (2003) Regulatory effects of G protein-coupled receptors on cardiac sarcolemmal Na^+/H^+ exchanger activity: signalling and significance. *Cardiovasc Res* **57:**942–952.

Barry GD, Le GT, and Fairlie DP (2006) Agonists and antagonists of protease activated receptors (PARs). *Curr Med Chem* **13:**243–265.

Belardinelli L, Shryock JC, and Fraser H (2006) Inhibition of the late sodium current as a potential cardioprotective principle: effects of the late sodium current inhibitor ranolazine. *Heart* **92(Suppl 4):**iv6–iv14.

Brette F and Orchard CH (2006) No apparent requirement for neuronal sodium channels in excitation-contraction coupling in rat ventricular myocytes. *Circ Res* **98:**667–674.

Chackalamannil S and Xia Y (2006) Thrombin receptor (PAR-1) antagonists as novel antithrombotic agents. *Expert Opin Ther Pat* **16:**493–505.

Coughlin SR (2000) Thrombin signalling and protease-activated receptors. *Nature* **407:**258–264.

Erlich JH, Boyle EM, Labriola J, Kovacich JC, Santucci RA, Fearns C, Morgan EN, Yun W, Luther T, Kojikawa O, et al. (2000) Inhibition of the tissue factor-thrombin pathway limits infarct size after myocardial ischemia-reperfusion injury by reducing inflammation. *Am J Pathol* **157:**1849–1862.

Fedida D, Orth PM, Hesketh JC, and Ezrin AM (2006) The role of late I and antiarrhythmic drugs in EAD formation and termination in Purkinje fibers. *J Cardiovasc Electrophysiol* **17 (Suppl 1):**S71–S78.

Glembotski CC, Irons CE, Krown KA, Murray SF, Sprenkle AB, and Sei CA (1993) Myocardial alpha-thrombin receptor activation induces hypertrophy and increases atrial natriuretic factor gene expression. *J Biol Chem* **268:**20646–20652.

Goldstein JA, Butterfield MC, Ohnishi Y, Shelton TJ, and Corr PB (1994) Arrhythmogenic influence of intracoronary thrombosis during acute myocardial ischemia. *Circulation* **90:**139–147.

Haigney MC, Lakatta EG, Stern MD, and Silverman HS (1994) Sodium channel blockade reduces hypoxic sodium loading and sodium-dependent calcium loading. *Circulation* **90:**391–399.

Herfst LJ, Potet F, Bezzina CR, Groenewegen WA, Le Marec H, Hoorntje TM, Demolombe S, Baro I, Escande D, Jongsma HJ, et al. (2003) Na^+ channel mutation leading to loss of function and non-progressive cardiac conduction defects. *J Mol Cell Cardiol* **35:**549–557.

Jacobsen AN, Du XJ, Lambert KA, Dart AM, and Woodcock EA (1996) Arrhythmogenic action of thrombin during myocardial reperfusion via release of inositol 1,4,5-triphosphate. *Circulation* **93:**23–26.

Jiang T, Kuznetsov V, Pak E, Zhang H, Robinson RB, and Steinberg SF (1996) Thrombin receptor actions in neonatal rat ventricular myocytes. *Circ Res* **78:**553–563.

Kiyosue T and Arita M (1989) Late sodium current and its contribution to action potential configuration in guinea pig ventricular myocytes. *Circ Res* **64:**389–397.

Lavi S, Lavi R, McConnell JP, Lerman LO, and Lerman A (2007) Lipoprotein-associated phospholipase a(2): review of its role as a marker and a potential participant in coronary endothelial dysfunction. *Mol Diagn Ther* **11:**219–226.

Makielski JC, Ye B, Valdivia CR, Pagel MD, Pu J, Tester DJ, and Ackerman MJ (2003) A ubiquitous splice variant and a common polymorphism affect heterologous expression of recombinant human SCN5A heart sodium channels. *Circ Res* **93:**821–828.

Maltsev VA, Sabbah HN, Higgins RS, Silverman N, Lesch M, and Undrovinas AI (1998) Novel, ultraslow inactivating sodium current in human ventricular cardiomyocytes. *Circulation* **98:**2545–2552.

Maltsev VA and Undrovinas AI (2006) A multi-modal composition of the late Na^+ current in human ventricular cardiomyocytes. *Cardiovasc Res* **69:**116–127.

Noble D and Noble PJ (2006) Late sodium current in the pathophysiology of cardiovascular disease: consequence of sodium-calcium overload. *Heart* **92:**iv1–iv5.

Park TH, McHowat J, Wolf RA, and Corr PB (1994) Increased lysophosphatidylcholine content induced by thrombin receptor stimulation in adult rabbit cardiac ventricular myocytes. *Cardiovasc Res* **28:**1263–1268.

Pinet C, Le Grand B, John GW, and Coulombe A (2002) Thrombin facilitation of voltage-gated sodium channel activation in human cardiomyocytes: implications for ischemic sodium loading. *Circulation* **106:**2098–2103.

Sabri A, Muske G, Zhang H, Pak E, Darrow A, Andrade-Gordon P, and Steinberg SF (2000) Signaling properties and functions of two distinct cardiomyocyte protease-activated receptors. *Circ Res* **86:**1054–1061.

Sabri A, Short J, Guo J, and Steinberg SF (2002) Protease-activated receptor-1-mediated DNA synthesis in cardiac fibroblast is via epidermal growth factor receptor transactivation: distinct PAR-1 signaling pathways in cardiac fibroblasts and cardiomyocytes. *Circ Res* **91:**532–539.

Saint DA (2006) The role of the persistent Na^+ current during cardiac ischemia and hypoxia. *J Cardiovasc Electrophysiol* **17 (Suppl 1):**S96–S103.

Sakmann BF, Spindler AJ, Bryant SM, Linz KW, and Noble D (2000) Distribution of a persistent sodium current across the ventricular wall in guinea pigs. *Circ Res* **87:**910–914.

Steinberg SF (2005) The cardiovascular actions of protease-activated receptors. *Mol Pharmacol* **67:**2–11.

Steinberg SF, Robinson RB, Lieberman HB, Stern DM, and Rosen MR (1991) Thrombin modulates phosphoinositide metabolism, cytosolic calcium, and impulse initiation in the heart. *Circ Res* **68:**1216–1229.

Strande JL, Hsu A, Su J, Fu X, Gross GJ, and Baker JE (2007) SCH 79797, a selective PAR1 antagonist, limits myocardial ischemia/reperfusion injury in rat hearts. *Basic Res Cardiol* **102:**350–358.

Undrovinas AI, Fleidervish IA, and Makielski JC (1992) Inward sodium current at resting potentials in single cardiac myocytes induced by the ischemic metabolite lysophosphatidylcholine. *Circ Res* **71:**1231–1241.

Undrovinas AI, Maltsev VA, Kyle JW, Silverman N, and Sabbah HN (2002) Gating of the late Na^+ channel in normal and failing human myocardium. *J Mol Cell Cardiol* **34:**1477–1489.

Valdivia CR, Chu WW, Pu J, Foell JD, Haworth RA, Wolff MR, Kamp TJ, and Makielski JC (2005) Increased late sodium current in myocytes from a canine heart failure model and from failing human heart. *J Mol Cell Cardiol* **38:**475–483.

Valdivia CR, Nagatomo T, and Makielski JC (2002) Late Na currents affected by alpha subunit isoform and beta1 subunit co-expression in HEK293 cells. *J Mol Cell Cardiol* **34:**1029–1039.

Woodcock EA, Matkovich SJ, and Binah O (1998) Ins(1,4,5)P3 and cardiac dysfunction. *Cardiovasc Res* **40:**251–256.

Wu L, Shryock JC, Song Y, and Belardinelli L (2006) An increase in late sodium current potentiates the proarrhythmic activities of low-risk QT-prolonging drugs in female rabbit hearts. *J Pharmacol Exp Ther* **316:**718–726.

Yan GX, Park TH, and Corr PB (1995) Activation of thrombin receptor increases intracellular Na^+ during myocardial ischemia. *Am J Physiol* **268:**H1740–H1748.

Address correspondence to: Alain Coulombe, INSERM U-621, 91 Blvd de l'Hôpital, 75634 Paris cedex 13, France. E-mail: alain.coulombe@chups.jussieu.fr